ARCHIVES OF MECHANICS
Arch. Mech. **75** (1-2), 213–242, 2023, DOI: 10.24423/aom.4144

A side-hinged paddle wavemaker

W. SULISZ, A. ZDOLSKA

Department of Wave Mechanics and Structural Dynamics,
Institute of Hydro-Engineering of Polish Academy of Sciences, 80-328 Gdańsk,
e-mail: sulisz@ibwpan.gda.pl (corresponding author), a.zdolska@ibwpan.gda.pl

Theoretical investigations were conducted to study the generation of transient nonlinear water waves by a novel side-hinged paddle wavemaker. A 3D nonlinear solution was derived in a semi-analytical form by applying eigenfunction expansions and FFT. The solution was applied to study the features of nonlinear waves generated by a side-hinged paddle wavemaker. The results show that nonlinear terms in the free-surface boundary conditions and in the kinematic wavemaker boundary condition imply the modification of wave profiles so that wave troughs are flattered and crests are getting steeper and interaction effects between waves in a wave train increase. Moreover, these terms imply the modification of a wave spectrum. A train of originally very narrow-banded waves changes its one-peak spectrum to a multi-peak one. Theoretical results are in a fairly good agreement with experimental data. A reasonable agreement is observed between predicted and measured time series of free-surface elevations and the amplitudes of the corresponding Fourier series. The investigations show that a side-hinged paddle wavemaker is an attractive wave generation system. Simple and reliable boundary condition at the paddle enables verification of advanced 3D nonlinear models and accurate physical modeling of many phenomena where high accuracy of incoming wave properties are important.

Key words: wave generation, side-hinged paddle wavemaker, three-dimensional numerical wave tank, nonlinear waves.

1. Introduction

A natural consequence of the progress achieved in coastal and offshore engineering is the expansion of hydraulic facilities which are indispensable to conduct physical modeling of wave-induced phenomena or current-affected processes. The development of modern laboratory equipment, in addition to the modeling of physical processes, is also necessary to conduct fundamental research and carry out verification of new analytical and numerical models. The development of new models is a natural consequence of increasing needs and new challenges facing coastal and offshore engineering. New laboratory facilities are vital for the sustainable development of coastal and offshore areas.

A linear wavemaker theory was first derived by Havelock [1] who applied Fourier integrals to develop a model for forced surface gravity waves. An explicit linear solution was first derived by Biesel and Suquet [2]. They applied eigenfunction expansions and derived a solution for the wave motions generated by both a piston and a hinged wavemaker. The solution derived by Biesel and Suquet [2] was extended by Hyun [3] to include hinged wavemakers of the variable draft. The modeling of the generation of waves in wave basins is far more complex than the modeling of the generation of waves in wave flumes. The first available models were derived for an infinitely long wavemaker by applying snake principles [4].

Laboratory experiments conducted by Ursell *et al.* [5], Galvin [6], Keating and Webber [7], or Patel and Ionnaou [8] have shown that the linear wavemaker theory provides satisfactory results for waves of very low steepness. When waves of finite amplitudes are generated by a sinusoidally moving wavemaker, it has been observed (Goda and Kikuya [9], Multer and Galvin [10], Iwagaki and Sakai [11]) that the propagating waves comprise of a primary wave and one or more secondary waves that are not predicted by the linear wavemaker solutions, which stimulated the advancement of nonlinear wavemaker theories.

A second-order nonlinear wavemaker theory was first derived by Fontanet [12] who developed a complete second-order solution in Lagrangian coordinates for waves generated by a sinusoidally moving plane wavemaker. Madsen [13] derived a solution in Eulerian coordinates for weakly nonlinear long waves generated by a sinusoidally moving piston wavemaker. Hudspeth and Sulisz [14], and Sulisz and Hudspeth [15], developed a complete second-order solution in Eulerian coordinates for a generic wavemaker. Their solution was later extended to waves generated in basins of finite width by Li and Williams [16], and basins of infinite width by Schaffer and Steenberg [17].

The process of the development of numerical models requires an appropriate verification procedure. Developed numerical models, in particular nonlinear wave models, must be verified by conducting comparisons of theoretical results with data obtained in laboratory experiments. Accurate verification of three-dimensional nonlinear wave models is not straightforward. The problem is that laboratory experiments, including experiments conducted in wave flumes or wave basins, have various limitations and require detailed knowledge on a generation system, limitations of applied equipment, potential side effects, etc. As a matter of fact, laboratory experiments have serious limitations, and data collected in wave flumes or wave basins are affected by wavemaker features, wave generation system, wave reflection and re-reflection, return currents, etc. (Hughes [18]). In many cases, especially cases related to the generation of waves in wave basins, discontinuities in wave generating system effect the formation and evolution of ripples on the free-surface and cause that it is difficult to generate good-quality

and undisturbed propagating waves. As a consequence, it is difficult to evaluate and eventually separate side effects, and to conduct precise experimental verifications of advanced theoretical models for which details of incoming wave properties are of fundamental importance. As a result, specific features of data collected in laboratory experiments as well as some side effects have to be taken into consideration in planning experiments and in the analysis of data collected during measurements.

An interesting and attractive alternative for the generation of three-dimensional nonlinear waves is a side-hinged planar wavemaker constructed in the wave flume of the Institute of Hydro-Engineering, the Polish Academy of Sciences, Gdańsk. Investigations conducted for a wide range of parameters and analyses of results confirm that the new generator is an attractive wave generation system. The side-hinged planar wavemaker, in addition to the precise verification of advanced three-dimensional nonlinear wave models, can be applied to conduct accurate investigations on nonlinear wave propagations in navigational channels, approaching harbor channels and basins, the interactions of nonlinear waves and cross-waves with structures, nonlinear cross-wave loads on ships including loads at berth, formation and development of cross waves, formation of wave resonance and seiches, sloshing phenomenon, selected slamming effects, etc. The wide range of the applicability of a side-hinged paddle wavemaker, easy access to this type of laboratory facilities, very low costs of laboratory experiments, and the fact that the wavemaker proposed in our study may be installed basically in all laboratories by changing the hinge of a flap, motivated theoretical investigations on waves generated by this type of a wavemaker. This is because a theoretical model provides insight into the effects of the free-surface boundary conditions and the kinematic wavemaker boundary condition on nonlinear waves and the physics of mechanically generated waves. This problem is vital for the interpretation and understanding of mechanically generated waves which are particular-type waves subject to nonlinear effects arising from the free-surface boundary conditions and the kinematic wavemaker boundary condition.

In this paper, theoretical and experimental investigations are conducted to study the generation of transient nonlinear water waves by a side-hinged paddle wavemaker. The boundary-value problem is formulated to describe the generation of nonlinear waves by a side-hinged flap wavemaker and a solution was achieved by applying a semi-analytical method. Then, theoretical investigations are conducted with emphasis on the features of nonlinear waves generated by a side-hinged wavemaker including the formation and development of cross waves. Next, the laboratory experiments are conducted and theoretical results are compared with experimental data for a wide range of wave parameters. Finally, conclusions arising from the analysis of theoretical results and experimental data are specified.

2. Theoretical formulation

2.1. Statement of the problem

We consider the generation of nonlinear water waves by a side-hinged paddle wavemaker in a wave basin. A right-hand Cartesian coordinate system was selected such that the xy plane is horizontal and coincides with the undisturbed free surface and z points vertically upwards (Fig. 1). It is assumed that:

a) the fluid is inviscid and incompressible,

b) the fluid motion is irrotational,

c) the bottom and the vertical-side walls are impervious.

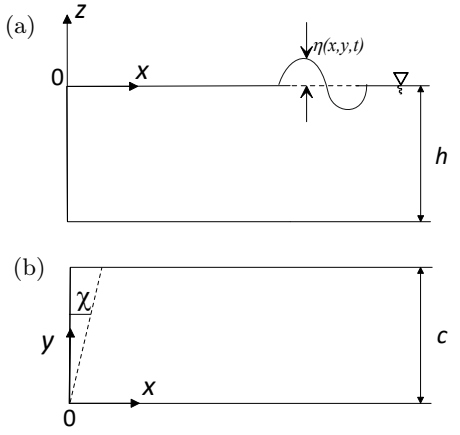

Fig. 1. Definitions sketch and coordinate systems; (a) side view and (b) top view.

In accordance with the assumptions, the velocity vector, $\boldsymbol{V}(x, y, z, t)$, may be computed from a velocity potential $\Phi(x, y, z, t)$:

$$\boldsymbol{V} = \nabla\Phi(x, y, z, t), \tag{2.1}$$

where $\nabla(\cdot)$ is the three-dimensional vector differential operator.

The fluid motion is governed by the continuity equation

$$\frac{\partial^2\Phi}{\partial x^2} + \frac{\partial^2\Phi}{\partial y^2} + \frac{\partial^2\Phi}{\partial z^2} = 0 \tag{2.2a}$$

and the Bernoulli equation

$$\frac{\partial\Phi}{\partial t} + \frac{1}{\rho}P + gz + \frac{1}{2}\left(\left(\frac{\partial\Phi}{\partial x}\right)^2 + \left(\frac{\partial\Phi}{\partial y}\right)^2 + \left(\frac{\partial\Phi}{\partial z}\right)^2\right) = 0, \tag{2.2b}$$

where ρ is the fluid mass density, P is the dynamic pressure, and g is the acceleration due to gravity.

The velocity potential, $\Phi(x, y, z, t)$, satisfies the Laplace equation:

$$\frac{\partial^2\Phi}{\partial x^2} + \frac{\partial^2\Phi}{\partial y^2} + \frac{\partial^2\Phi}{\partial z^2} = 0, \quad x \geq \chi(y, z, t),\ -h \leq z \leq \eta(x, y, t) \tag{2.3a}$$

with the kinematic boundary condition on the free surface:

$$\frac{\partial\eta}{\partial t} + \frac{\partial\Phi}{\partial x}\frac{\partial\eta}{\partial x} + \frac{\partial\Phi}{\partial y}\frac{\partial\eta}{\partial y} - \frac{\partial\Phi}{\partial z} = 0, \quad z = \eta(x, y, t),\ x \geq \chi(y, z, t), \tag{2.3b}$$

the dynamic boundary condition on the free surface:

$$\frac{\partial\Phi}{\partial t} + g\eta + \frac{1}{2}\left(\left(\frac{\partial\Phi}{\partial x}\right)^2 + \left(\frac{\partial\Phi}{\partial y}\right)^2 + \left(\frac{\partial\Phi}{\partial z}\right)^2\right) = 0, \quad z = \eta(x, y, t),\ x \geq \chi(y, z, t), \tag{2.3c}$$

the kinematic boundary condition on the wavemaker

$$\frac{\partial\chi}{\partial t} + \frac{\partial\Phi}{\partial y}\frac{\partial\chi}{\partial y} + \frac{\partial\Phi}{\partial z}\frac{\partial\chi}{\partial z} - \frac{\partial\Phi}{\partial x} = 0, \quad x = \chi(y, z, t),\ -h \leq z \leq \eta(x, y, t), \tag{2.3d}$$

the kinematic boundary condition at the walls:

$$\Phi_y = 0, \quad y = 0, c \quad x \geq \chi(y, z, t), \tag{2.3e}$$

and the kinematic boundary condition at the bottom of the basin:

$$\Phi_z = 0, \quad z = -h, \quad x \geq \chi(y, z, t), \tag{2.3f}$$

where h is the water depth, c is the basin width, and χ is the wavemaker displacement. In addition, the velocity potential must satisfy a boundary condition at infinity and initial conditions (Wehausen [19], Kinsmann [20]).

A solution may be achieved by expanding the kinematic free-surface boundary condition (2.3b), the dynamic free-surface boundary condition (2.3c), and the kinematic wavemaker boundary condition (2.3d) in a Taylor series about a mean position,

$$\sum_{n=0}^{\infty} \frac{\eta^n}{n!}\frac{\partial^n}{\partial z^n}\left(\frac{\partial\eta}{\partial t} + \frac{\partial\Phi}{\partial x}\frac{\partial\eta}{\partial x} + \frac{\partial\Phi}{\partial y}\frac{\partial\eta}{\partial y} - \frac{\partial\Phi}{\partial z}\right) = 0, \quad z = 0,\ x \geq 0, \tag{2.4a}$$

$$\sum_{n=0}^{\infty} \frac{\eta^n}{n!}\frac{\partial^n}{\partial z^n}\left\{\frac{\partial\Phi}{\partial t} + g\eta + \frac{1}{2}\left(\left(\frac{\partial\Phi}{\partial x}\right)^2 + \left(\frac{\partial\Phi}{\partial y}\right)^2 + \left(\frac{\partial\Phi}{\partial z}\right)^2\right)\right\} = 0, \quad z = 0,\ x \geq 0, \tag{2.4b}$$

$$\sum_{n=0}^{\infty} \frac{\chi^n}{n!} \frac{\partial^n}{\partial x^n} \left(\frac{\partial \chi}{\partial t} + \frac{\partial \Phi}{\partial y}\frac{\partial \chi}{\partial y} + \frac{\partial \Phi}{\partial z}\frac{\partial \chi}{\partial z} - \frac{\partial \Phi}{\partial x} \right) = 0, \quad x = 0,\ -h \le z \le 0. \tag{2.4c}$$

By applying (2.4) to (2.3) and collecting terms up to the second order in a wave amplitude one obtains the following boundary-value problem:

$$\frac{\partial^2 \Phi}{\partial x^2} + \frac{\partial^2 \Phi}{\partial y^2} + \frac{\partial^2 \Phi}{\partial z^2} = 0, \quad x \ge 0, -h \le z \le 0, \tag{2.5a}$$

$$\frac{\partial \eta}{\partial t} - \frac{\partial \Phi}{\partial z} - \eta \frac{\partial^2 \Phi}{\partial z^2} + \frac{\partial \Phi}{\partial x}\frac{\partial \eta}{\partial x} + \frac{\partial \Phi}{\partial y}\frac{\partial \eta}{\partial y} = 0, \quad z = 0,\ x \ge 0, \tag{2.5b}$$

$$\frac{\partial \Phi}{\partial t} + g\eta + \frac{1}{2}\left(\left(\frac{\partial \Phi}{\partial x} \right)^2 + \left(\frac{\partial \Phi}{\partial y} \right)^2 + \left(\frac{\partial \Phi}{\partial z} \right)^2 \right) + \eta \frac{\partial^2 \Phi}{\partial z \partial t} = 0, \quad z = 0,\ x \ge 0, \tag{2.5c}$$

$$\frac{\partial \chi}{\partial t} + \frac{\partial \Phi}{\partial y}\frac{\partial \chi}{\partial y} + \frac{\partial \Phi}{\partial z}\frac{\partial \chi}{\partial z} - \frac{\partial \Phi}{\partial x} - \chi \frac{\partial^2 \Phi}{\partial x^2} = 0,\ x = 0\,; \quad -h \le z \le 0, \tag{2.5d}$$

$$\frac{\partial \Phi}{\partial z} = 0, \quad z = -h,\ x \ge 0. \tag{2.5e}$$

Moreover, the velocity potential must satisfy a boundary condition at infinity and initial conditions.

The boundary-value problem describes the generation of nonlinear waves in a basin by a side-hinged paddle wavemaker. A solution must properly describe nonlinear effects arising from the free-surface boundary conditions and the kinematic wavemaker boundary condition. Widely-applied weakly nonlinear wave models do not satisfy the boundary-value problem, (2.5a–e). This is because classical nonlinear wave models do not satisfy the kinematic wavemaker boundary condition, (2.5d). Mechanically generated waves are specific-type waves and their description require new approaches and novel solution techniques.

2.2. Solution

The boundary-value problem, (2.5), is solved by applying eigenfunction expansions and a time-stepping procedure supported by FFT. This method has been shown to be an efficient technique in the modeling of the propagation and transformation of nonlinear waves (SULISZ and PAPROTA [21, 22]). The application of the eigenfunction expansion method and FFT is very attractive from a computational point of view.

It is customary in the boundary-value problems with inhomogeneous boundary conditions to decompose the solution into complementary components. Accordingly, the velocity potential, Φ, may be expressed as a linear combination of two velocity potentials given by:

$$\Phi = \Phi_f + \Phi_w, \tag{2.6a}$$

where

$$\Phi_f(x,y,z,t) = \sum_{m=0}\sum_{n=0} A_{mn}\frac{\cosh\lambda_{mn}(z+h)}{\cosh\lambda_{mn}h}\cos\lambda_{m0}x\cos\lambda_{0n}y, \tag{2.6b}$$

$$\Phi_w(x,y,z,t) = B_{00}((x-b)^2-(z+h)^2) + \sum_{m=0}\sum_{n=0}(1-\delta_{00mn})B_{mn}\frac{\cosh\mu_{mn}(x-b)}{\cosh\mu_{mn}b}\cos\mu_{0n}y\cos\mu_{m0}(z+h), \tag{2.6c}$$

$$\eta(x,y,t) = \sum_{m=0}\sum_{n=0} a_{mn}\cos\lambda_{m0}x\cos\lambda_{0n}y \tag{2.6d}$$

and where the eigenvalues can be determined from

$$\lambda_{mn} = \pi\sqrt{m^2/b^2+n^2/c^2}, \tag{2.6e}$$

$$\mu_{mn} = \pi\sqrt{m^2/h^2+n^2/c^2}, \tag{2.6f}$$

in which A_{mn}, B_{mn}, a_{mn} are unknown coefficients, c is a basin width, and b is the length of the basin that is assumed to be sufficiently large to prevent wave reflection.

The unknown coefficients of the solution may be determined from the boundary conditions by applying the Fourier method (KANTOROVICH and KRILOV [23]) and the Adams–Bashford–Moulton predictor-corrector method (PRESS *et al.* [24]). The applied solution technique enables the prediction of the free-surface elevation, η, and the velocity potential, Φ, from their time derivatives. Accordingly, the coefficients a_{mn} and A_{mn} are determined by applying in an iterative procedure (2.5b) and (2.5c) and the Adams–Bashford predictor

$$f_{n+1} = f_n + \frac{\Delta t}{24}(55f'_n - 59f'_{n-1} + 37f'_{n-2} - 9f'_{n-3}) \tag{2.7a}$$

combined with the Adams–Moulton corrector

$$f_{n+1} = f_n + \frac{\Delta t}{24}(9f'_{n+1} + 19f'_n - 5f'_{n-1} + f'_{n-2}), \tag{2.7b}$$

where f' is the time derivative of f.

The coefficients B_{mn}, $m = 0,1,2,\ldots$, $n = 0,1,2,\ldots$ are determined by applying (2.5d) and FFT.

The derived solution describes the generation of nonlinear progressive waves and cross waves in the time domain. The evanescent modes play an important role in the descriptions and modeling of wavemaker problems. The evanescent modes are explicitly present in frequency-domain solutions and contribute to a far-field solution. Of course, the evanescent modes are also present in time-domain solutions, however, in a non-explicit form. They are incorporated in the

time-domain terms of a final solution. The solution is very efficient and may be applied to predict wave generation and propagation even in large wave basins. The applicability range of the solution may further be increased by the implementation of wave absorbers in a wave basin (Sulisz [25]). The introduction of an absorber also enables the modeling of partial wave reflection that is observed in real wave basins.

3. Theoretical results

The derived solution was applied to analyze the generation of transient nonlinear water waves by a side-hinged paddle wavemaker. The analysis is conducted for the time history of the wavemaker displacement presented for a basic amplification factor and $x = 0$, $y = c$ in Fig. 2. The wavemaker generation program comprises four basic wave periods corresponding to the ratio of the wavelength, L, to the water depth, h, equal to $L/h = 4, 6, 8$, and 12. For each basic wave period, the wavemaker generates wave trains corresponding to low, moderate, and steep waves. This is included in the generation program to investigate nonlinear effects arising from the generation and propagation of waves in a wave basin with a side-hinged paddle wavemaker. The calculations are conducted for the basin of width $c/h = 1.5$ and the results are presented for $x/h = 5$, $y/h = 0.75$.

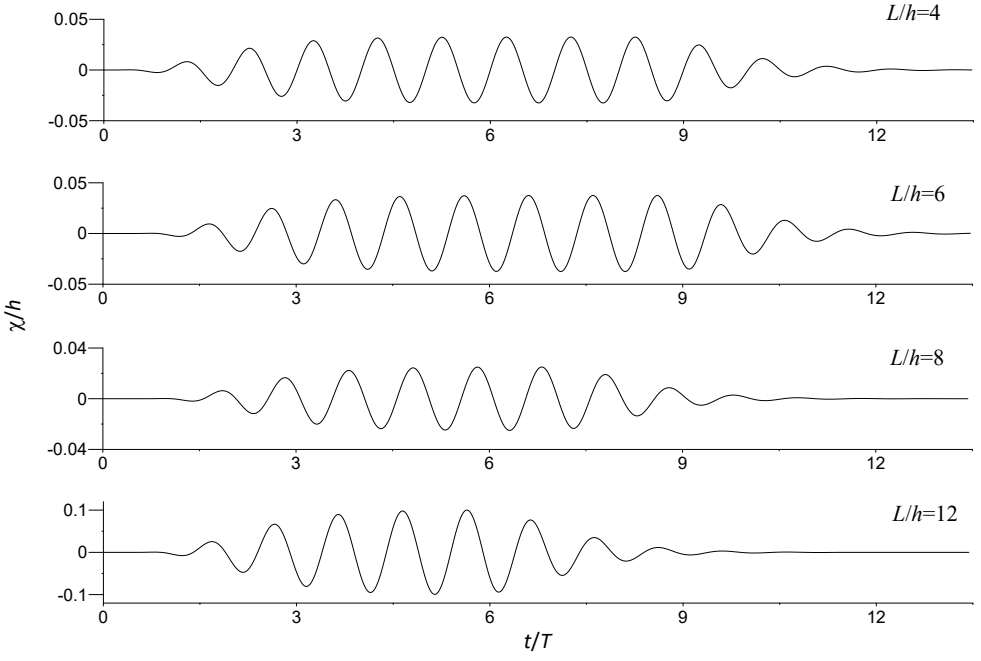

Fig. 2. Time history of the wavemaker displacement.

The results are analyzed with the emphasis on the effect of wave frequencies and wave steepness on the generation and propagation of a wave train in a wave basin with a side-hinged paddle wavemaker. The wave profile, the wave energy spectrum, and the evolution of wave profile arising from the generation, propagation, and transformation of nonlinear wave components in wave trains are analyzed. The results obtained by applying the nonlinear model are compared with the outcome of the analytical solution derived for the generation of linear waves by a side-hinged paddle wavemaker. The derived analytical solution and the comparisons conducted with the results obtained by applying the nonlinear model help to evaluate the effects of nonlinear terms included in boundary conditions on wave profile, wave spectrum, and the evolution of wave profile and wave spectrum due to the generation, propagation, and transformation of nonlinear waves in a wave basin with a side-hinged paddle wavemaker.

First, the derived model is applied to predict the generation and propagation of waves of small amplitudes. The application of the model to waves of low steepness enables us to verify the numerical scheme because the outcome of the model should be basically the same as the results provided by the analytical solution derived within the frame of linear wave theory. The results corresponding to waves of low steepness are shown in Fig. 3. The plots in Fig. 3 also show the outcome of the Fourier analysis that was applied to obtain an amplitude wave spectrum and information on wave frequency components. The results predicted by the derived model are in good agreement with the analytical solution. The discrepancies between the outcome of the linear and nonlinear models increase with increasing wavelength. In fact, increasing discrepancies between linear and nonlinear models with increasing wavelength is an expected result related to general features of water waves.

A real challenge for the modeling of the generation of water waves in wave flumes and wave basins is the prediction of waves for large wavemaker displacements. The advantages of the derived nonlinear model can be demonstrated by applying it to waves of higher steepness for which a linear wave theory cannot provide satisfactory results. The outcomes of calculations conducted for waves of moderate steepness and steep waves are presented in Figs. 4 and 5. The results for waves of moderate steepness and steep waves correspond to the time history of the wavemaker displacement presented in Fig. 2 multiplied by an amplification factor two and four, respectively. The plots in Figs. 4 and 5 also show the time series of the free-surface elevation predicted by applying an analytical solution derived within the frame of linear wave theory. Moreover, the plots show the outcome of the Fourier analysis that was applied to obtain amplitude wave spectrums and information on wave frequency components.

The results presented in Figs. 4 and 5 indicate a need to apply nonlinear approaches in the modeling of the generation and propagation of waves in a wave

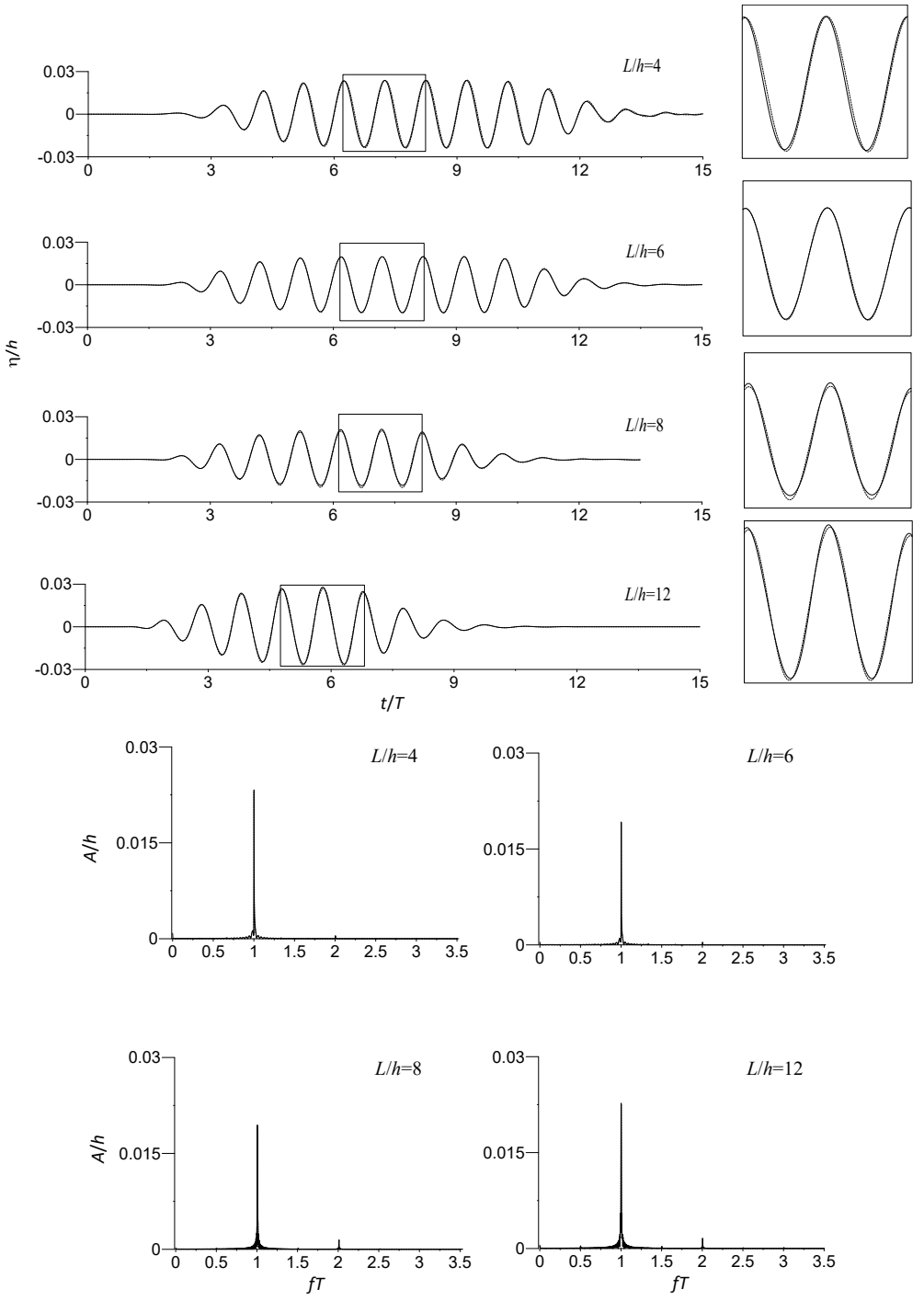

Fig. 3. Free-surface elevation and amplitudes of Fourier series for waves of low steepness, — nonlinear theory, - - - linear theory.

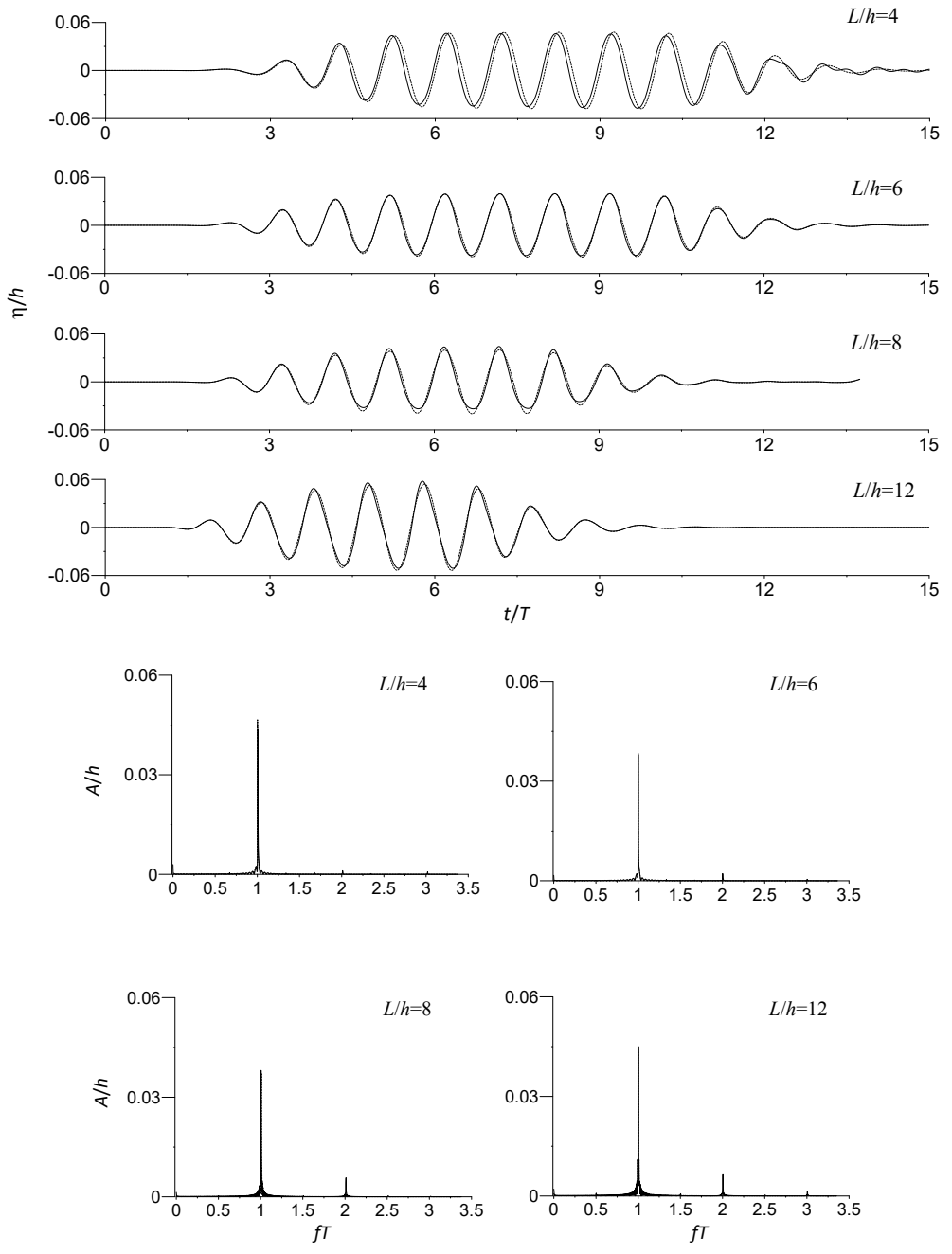

FIG. 4. Free-surface elevation and amplitudes of Fourier series for waves of moderate steepness, — nonlinear theory, - - - linear theory.

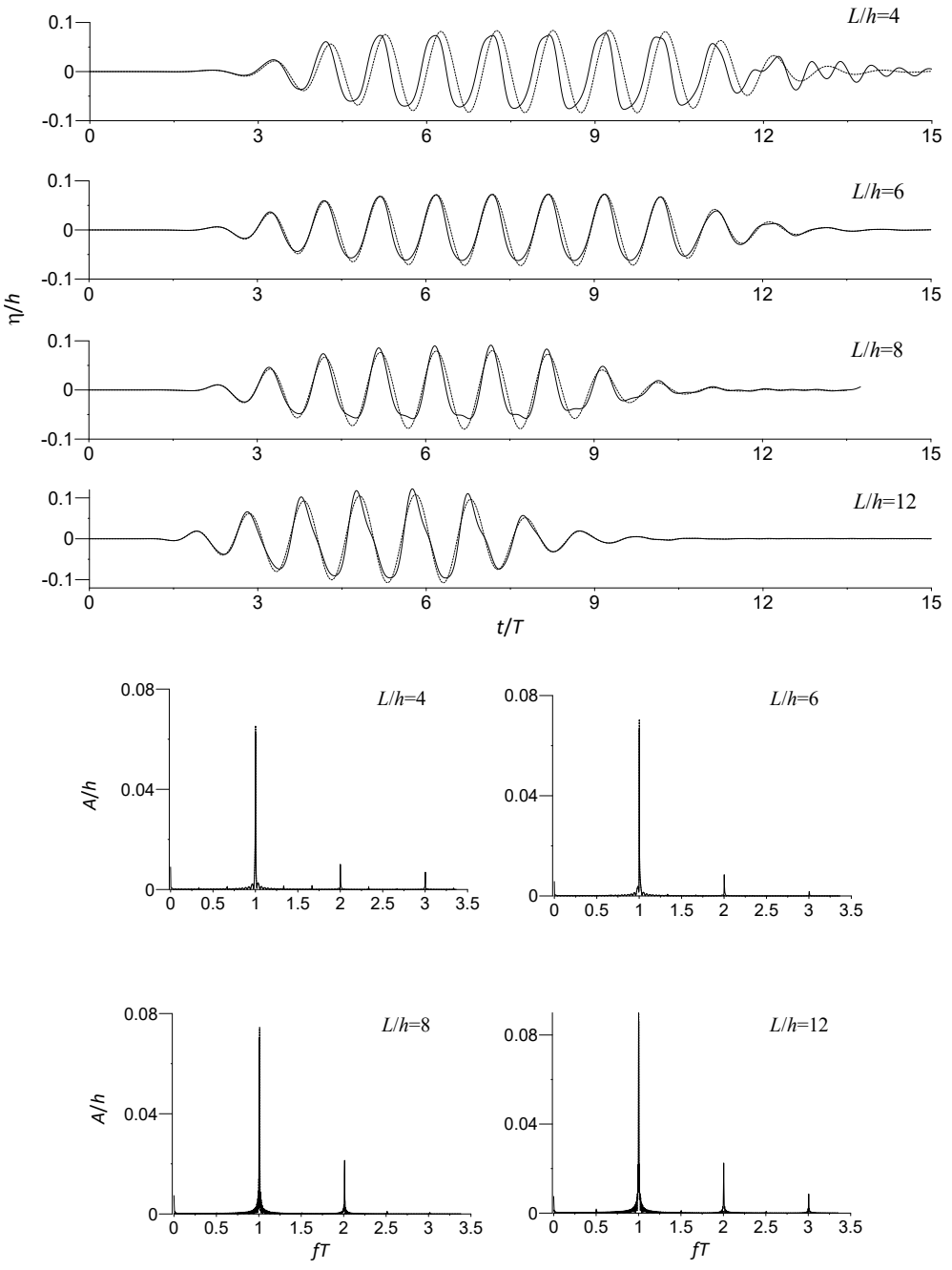

Fig. 5. Free-surface elevation and amplitudes of Fourier series for steep waves, — nonlinear theory, --- linear theory.

basin with a side-hinged paddle wavemaker. The application of the nonlinear model has a significant effect on a wave profile. For waves of low steepness, the nonlinear wave effects and effects associated with the interaction of water waves in a wave train are of secondary importance and the linear wavemaker solution may be applied to predict water waves generated in a wave basin. For the larger amplitudes of the wavemaker oscillations, generated waves are higher, which implies stronger nonlinear wave effects and the interactions between waves in a wave train are no longer negligible. This also causes the modification of a wave profile – wave troughs are flattered and crests are getting steeper. The discrepancies between a wave profile predicted by applying the linear and nonlinear models increase with increasing wavelength and become significant for long waves which profile become more and more cnoidal with increasing wavelength. The results presented in Figs. 4 and 5 also show that the application of the nonlinear model has a significant effect on the shape of a wave spectrum for moderate and large wavemaker displacements. A train of originally very narrow-banded waves changes its one-peak spectrum to a multi-peak one when a wavemaker amplitude increases.

The nonlinear waves imply changes of wave profiles and wave spectrum, and lead to wave instabilities in intermediate and deep waters. Mechanically generated waves are specific-type waves subject to nonlinear effects arising from two sources. Namely, these waves are subject to nonlinear effects arising from the free-surface boundary conditions and the kinematic wavemaker boundary condition. An insight into the contribution of the nonlinear terms present in the boundary conditions illustrates the results in Fig. 6. The plots in Fig. 6 illustrate the importance of nonlinear terms in the free-surface boundary conditions and in the kinematic wavemaker boundary condition on the final solution. The results show that the contributions of nonlinear terms present in the kinematic wavemaker boundary condition are of secondary importance for a final solution. The low effects of the nonlinear terms in the kinematic wavemaker boundary condition on a solution are the advantage of a side-hinged paddle wavemaker because nonlinear wave effects disturb physical modeling of numerous processes including wave-induced transport, sediment transport, etc. Often, nonlinear wave effects may drastically disturb or even exclude physical modeling conducted in wave flumes or wave basins by altering or completely deforming a designed wave spectrum.

There is an advantage of including the limited number of waves in a wave train for potential readers and users, who may easily verify their analytical and numerical solutions by applying presented input data and results, because it is easy to prepare input files from presented results by digitizing plots and run derived models on personal computers. The presentation of the limited number of waves in the wave train is a recognized standard (SULISZ and PAPROTA [21, 22];

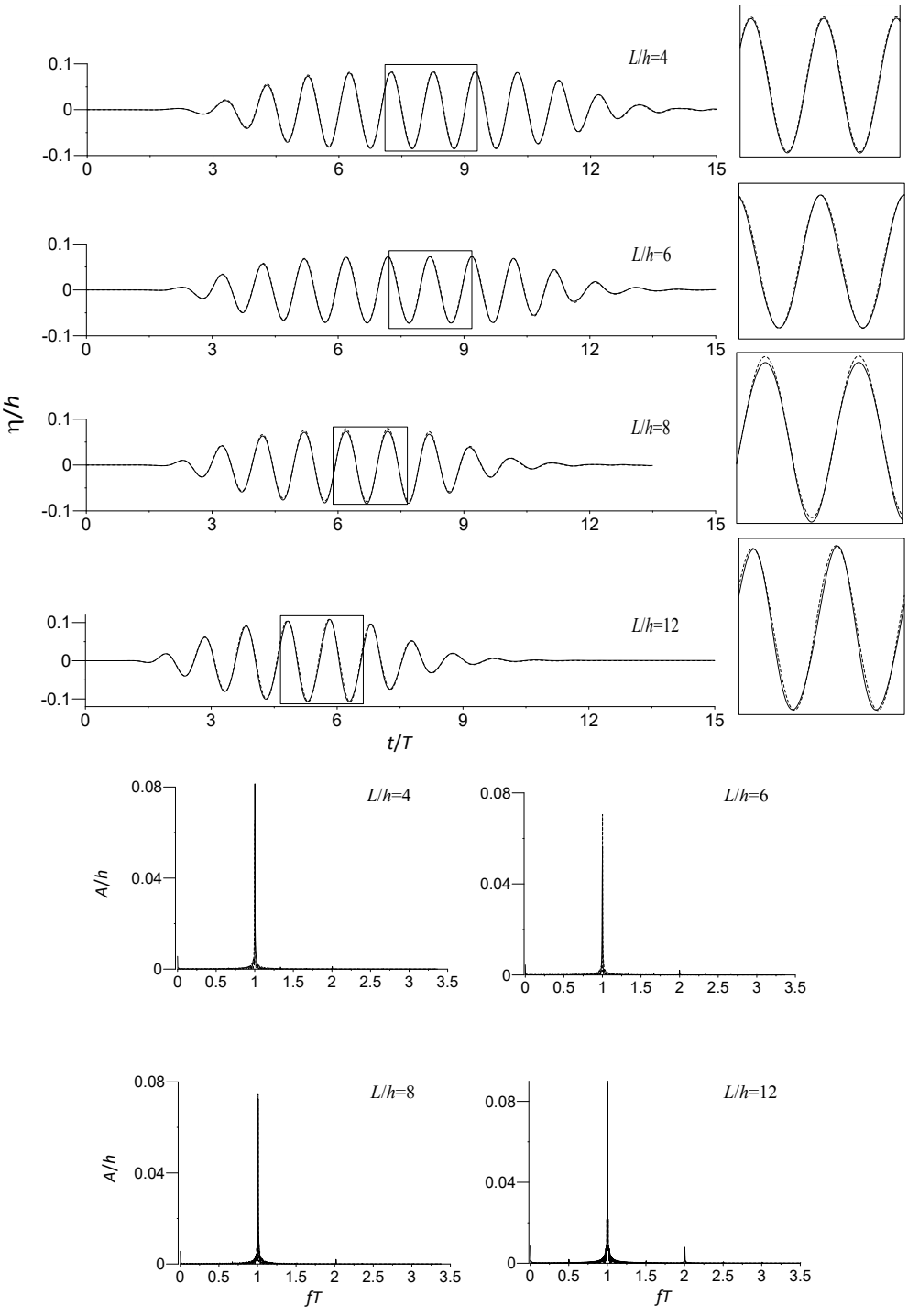

Fig. 6a. Free-surface elevation and amplitudes of Fourier series for steep waves, — nonlinear wavemaker and linear free-surface boundary conditions, --- linear theory.

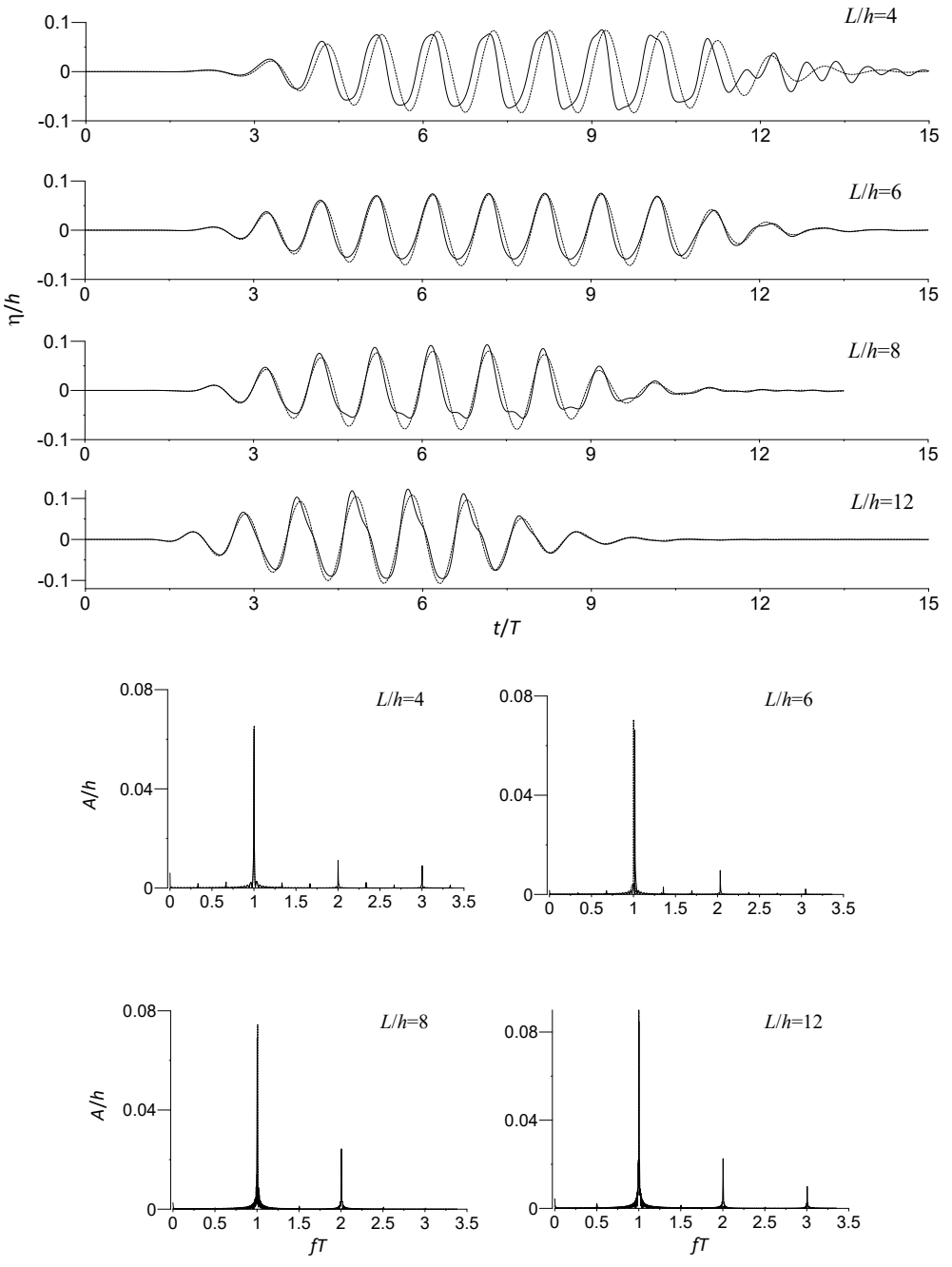

FIG. 6b. Free-surface elevation and amplitudes of Fourier series for steep waves, — nonlinear free-surface and linear wavemaker boundary conditions, --- linear theory.

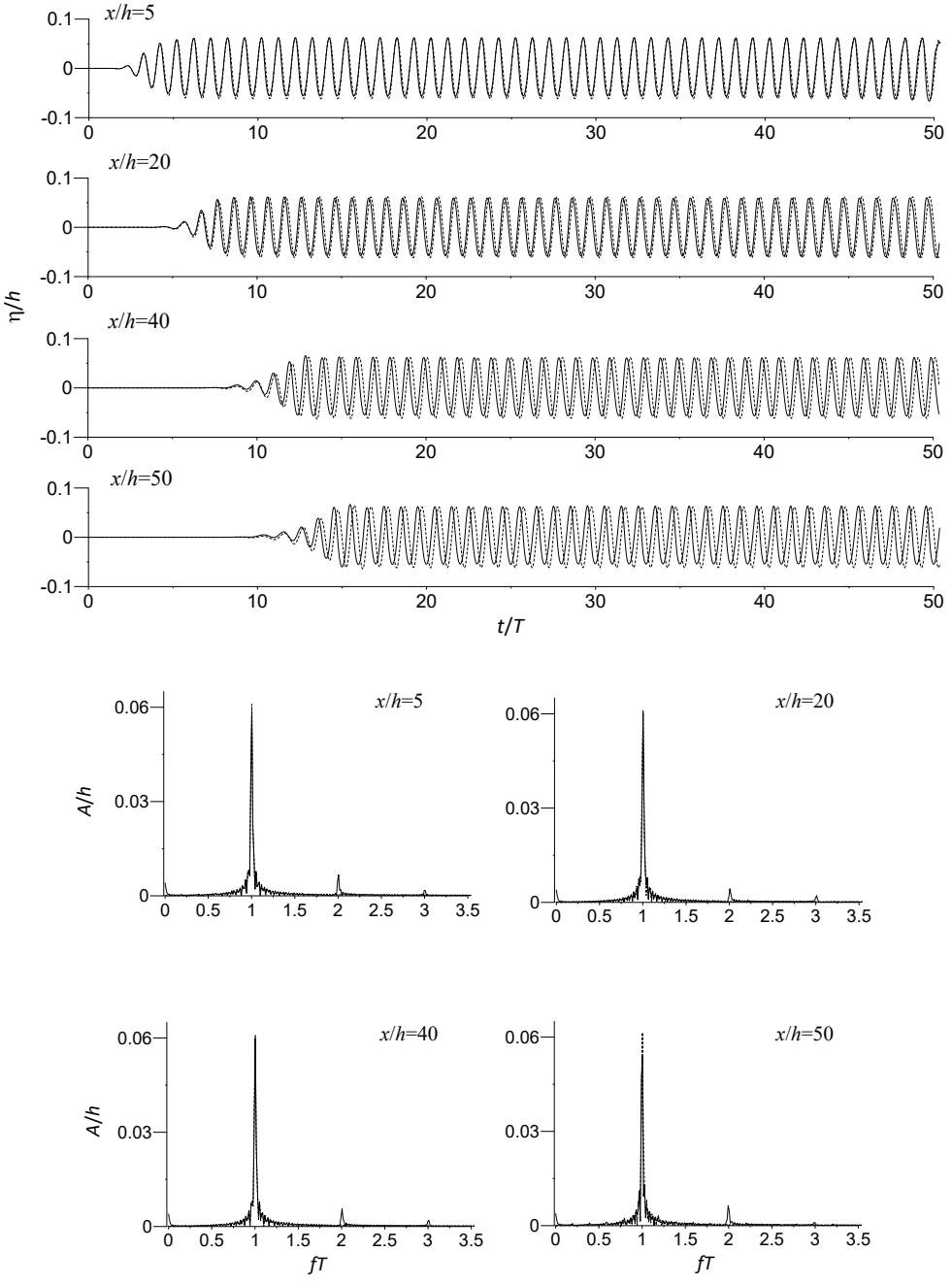

Fig. 7. Free-surface elevations and amplitudes of Fourier series for long wave trains, $L/h = 6$, — nonlinear theory, --- linear theory.

PAPROTA and SULISZ [26]). However, for completes, Fig. 7 shows the results obtained for a large number of waves in a wave train at different locations of a long wave basin. The analysis of the results shows that the outcome of the model and conclusions are the same as for the limited number of waves in a wave train.

Additional calculations and analysis show that widely-applied weakly nonlinear wavemaker models cannot properly describe the wave profile and wave spectrum when wave steepness exceeds low wave steepness limits. The analysis shows that for waves of moderate steepness and relatively steep waves the discrepancies between results obtained by the application of weakly nonlinear wavemaker models and nonlinear approaches are becoming significant especially in shallow and deep waters. This is because the weakly nonlinear wavemaker models are based on a perturbation theory that has a number of limitations. As a consequence, the free-surface boundary conditions, the kinematic wavemaker boundary condition, the nonlinear interactions of wave components in wave trains, and the evolution of wave energy spectrum are not described with sufficient accuracies. The prediction of the generation and propagation of waves of moderate steepness and steep waves requires the application of nonlinear wavemaker models.

4. Experimental verification

4.1. Laboratory experiments

Laboratory experiments were conducted in the wave flume at the Institute of Hydro-Engineering, the Polish Academy of Sciences, Gdańsk. The wave flume is 64 m long, 0.6 m wide and 1.4 m deep and it is equipped with a programmable side-hinged paddle wavemaker. Two porous wave absorbers are supplied at both

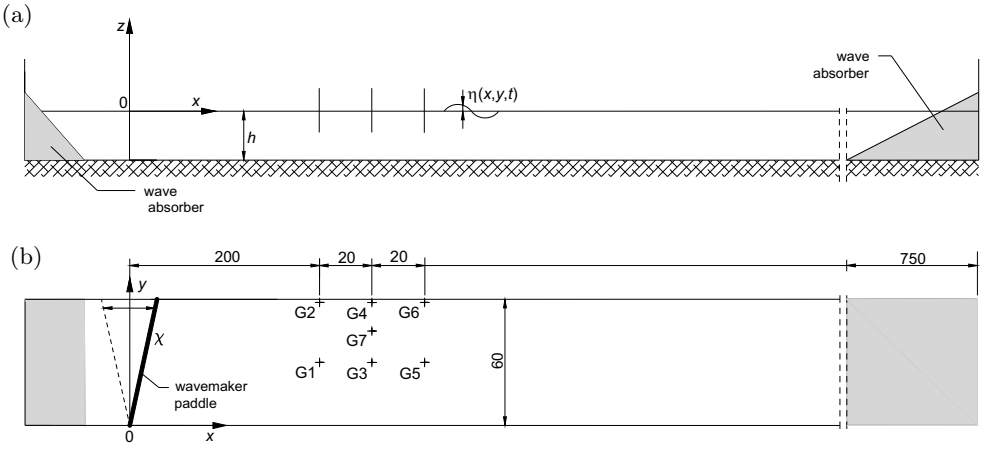

FIG. 8. The wave flume; (a) the side view and (b) the top view.

ends of the wave flume (Fig. 8). The experiments were conducted at the water depth $h = 0.4\,\mathrm{m}$. The wavemaker generated wave trains of dominant frequencies corresponding to the wave lengths of 4.0 m, 2.4 m, and 1.2 m. To minimize side effects arising from the development of noise in the wave basin, the wave-generator motion was started and terminated by applying a pre-tested ramp function. Experimental verifications were conducted for free-surface elevations, $\eta(x, y, t)$.

The free-surface elevations were recorded by a system of resistance-type wave gauges. The system consisted of seven wave gauges G1: $x = 2.0\,\mathrm{m}$, $y = 0.3\,\mathrm{m}$; G2: $x = 2.0\,\mathrm{m}$, $y = 0.58\,\mathrm{m}$; G3: $x = 2.2\,\mathrm{m}$, $y = 0.3\,\mathrm{m}$; G4: $x = 2.2\,\mathrm{m}$, $y = 0.58\,\mathrm{m}$; G5: $x = 2.4\,\mathrm{m}$, $y = 0.3\,\mathrm{m}$; G6: $x = 2.4\,\mathrm{m}$, $y = 0.58\,\mathrm{m}$; G7: $x = 2.2\,\mathrm{m}$, $y = 0.45\,\mathrm{m}$. The free-surface elevation was sampled 200 times per second.

4.2. Experimental and theoretical comparisons

Theoretical results of the free-surface elevations calculated by applying the derived three-dimensional nonlinear model were compared with the time series of the free-surface elevations measured by wave gauges. The comparisons are presented in Figs. 9–12. The free-surface elevation was calculated by applying the wavemaker displacement recorded at $y/h = 1.4$ and the amplitudes of wave components in a wave train were determined by the standard Fourier analysis. The calculations were conducted at the positions of wave gauges considered in laboratory experiments. For completes, additional comparisons of the theoretical results with experimental data are presented for a long wave train. The plots in Figs. 9–12 show a fairly good agreement between theoretical results predicted by the nonlinear model and the experimental data. A reasonable agreement is observed between predicted and measured time series of the free-surface elevations and the amplitudes of the corresponding Fourier series. The plots also show that wave phases predicted by applying the theoretical models are in reasonable agreement with experimental data. Moreover, the model predicts fairly well the multi-peak spectrum characteristic for nonlinear wave components.

The comparisons of theoretical results with experimental data also show that the derived model predicts the formation and development of cross-waves with reasonable accuracy. A side-hinged paddle wavemaker generates a plane wave and cross waves. For relatively long waves generated in a wave basin cross waves decay with increasing the distance from the wavemaker and changes of the wave amplitude across a basin are low. However, for shorter waves, at least one cross-wave mode does not decay with increasing the distance from the wavemaker and a wave amplitude changes its magnitude across the wave basin. The rate of the contribution of cross waves to the free-surface oscillations may be easily controlled by increasing or decreasing water depth in a wave basin, which is the significant advantage of a side-hinged paddle wavemaker concept.

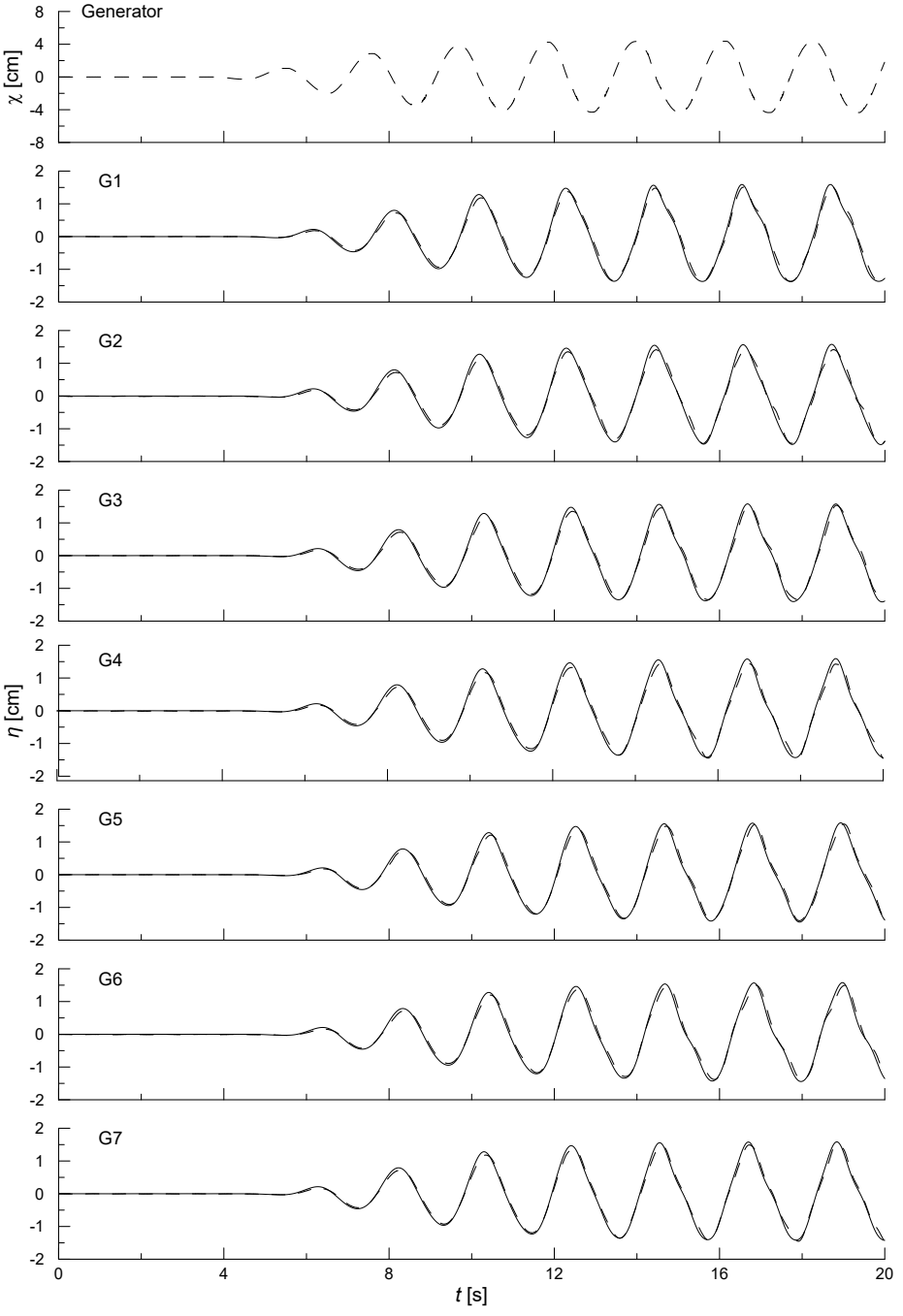

FIG. 9a. Predicted and measured free-surface elevation for $L/h = 10$, — theoretical results, --- experimental data.

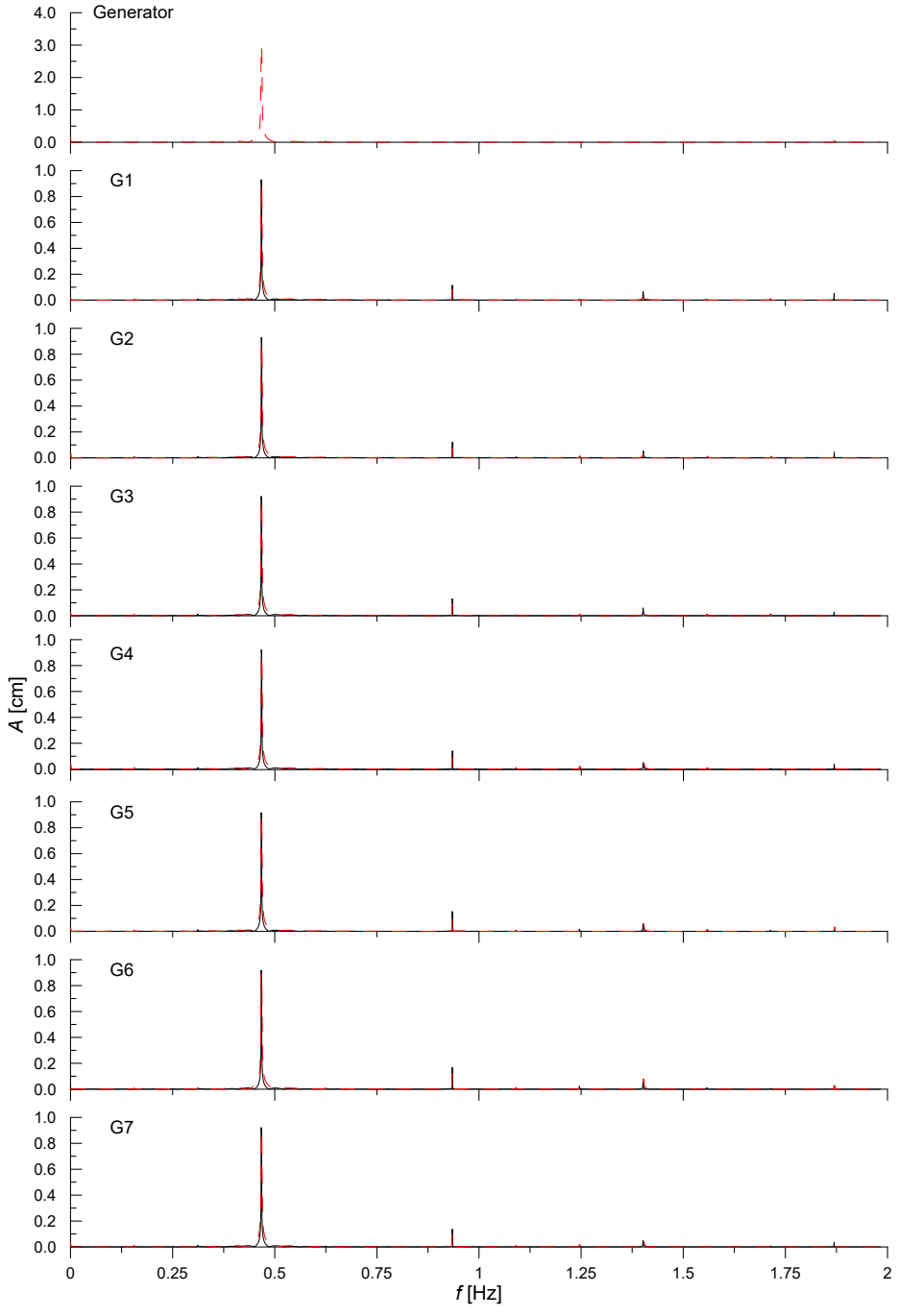

Fig. 9b. Amplitudes of Fourier series for $L/h = 10$, — theoretical results, - - - experimental data.

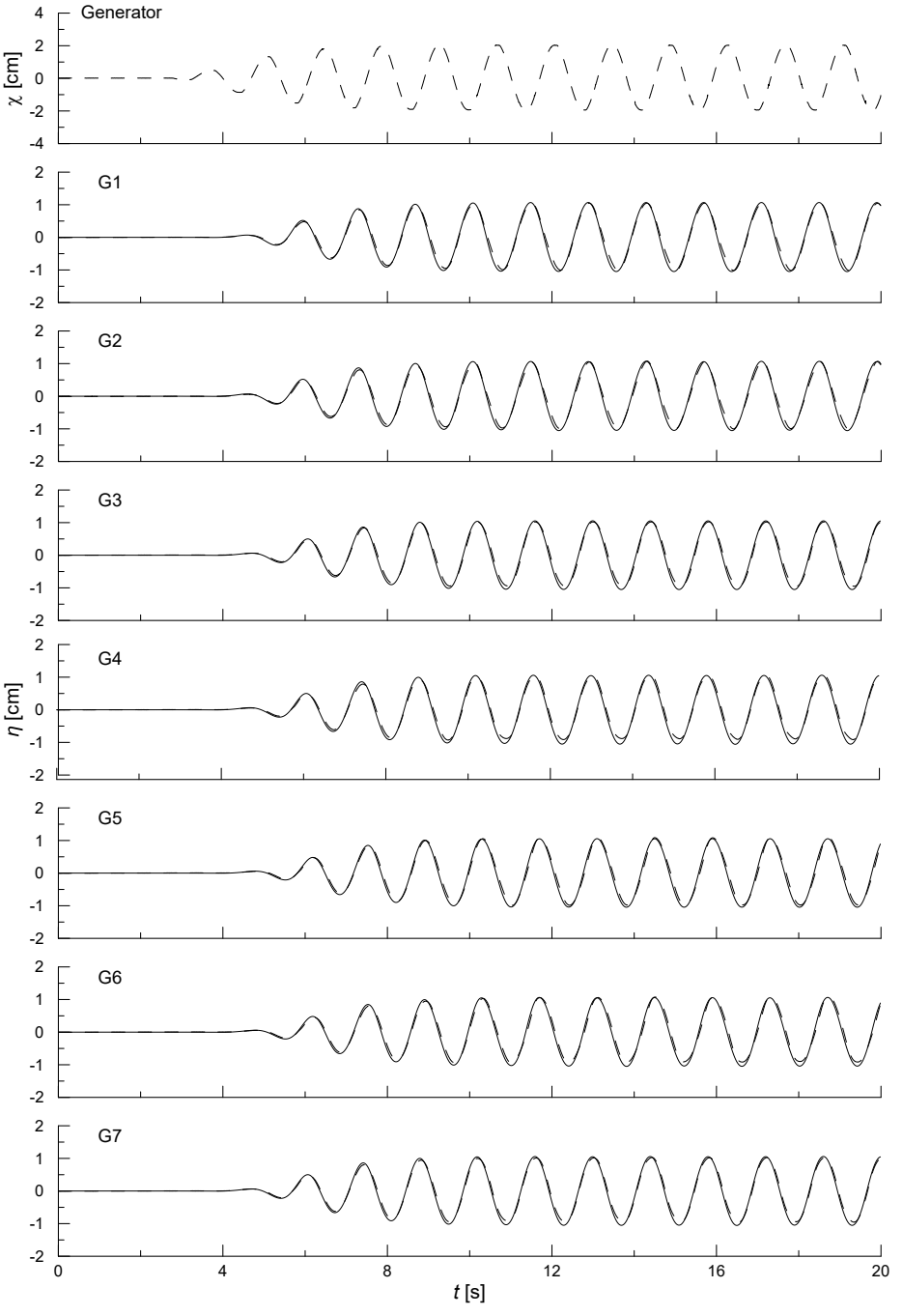

FIG. 10a. Predicted and measured free-surface elevation for $L/h = 6$, — theoretical results, --- experimental data.

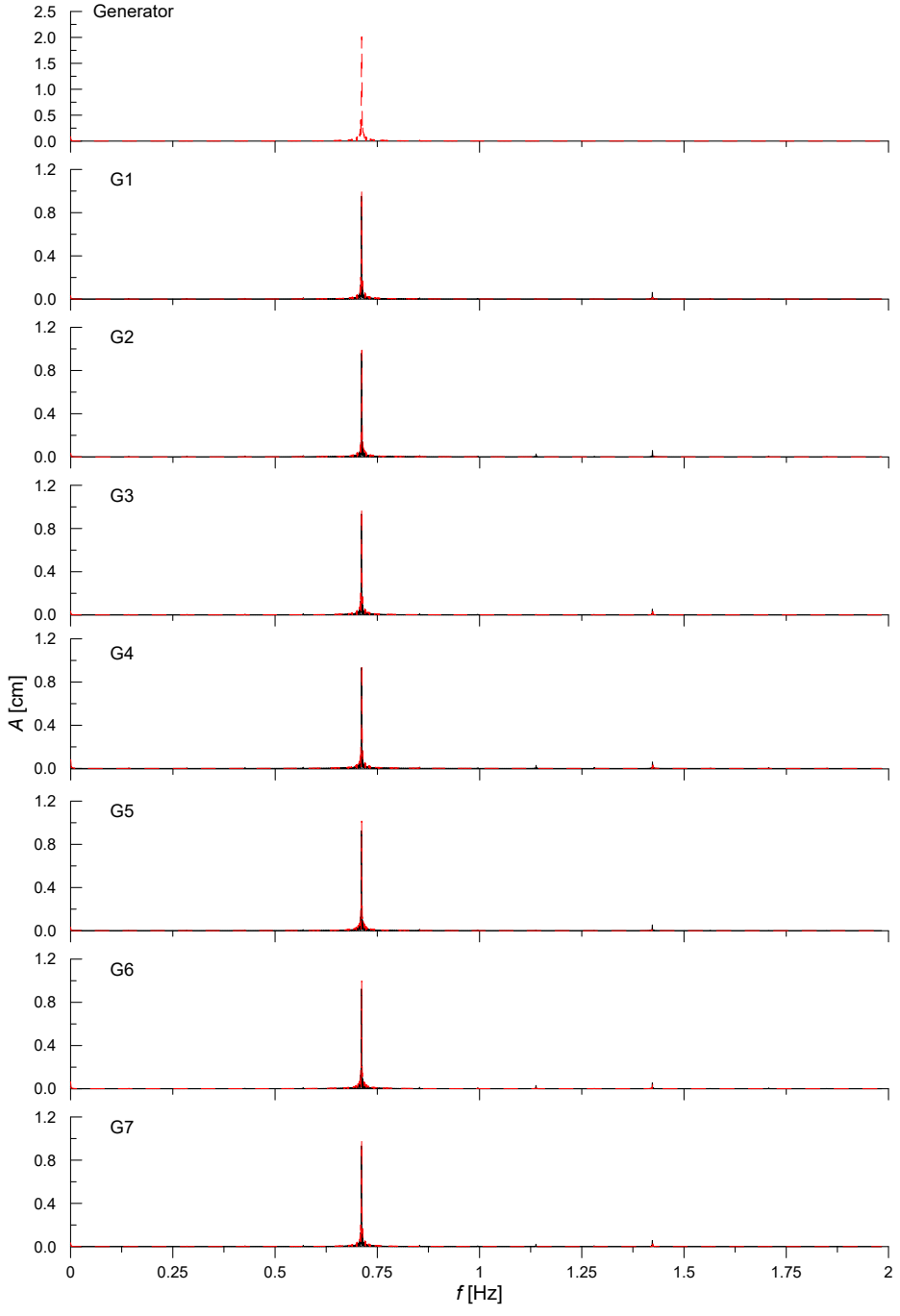

Fig. 10b. Amplitudes of Fourier series for $L/h = 6$, — theoretical results, --- experimental data.

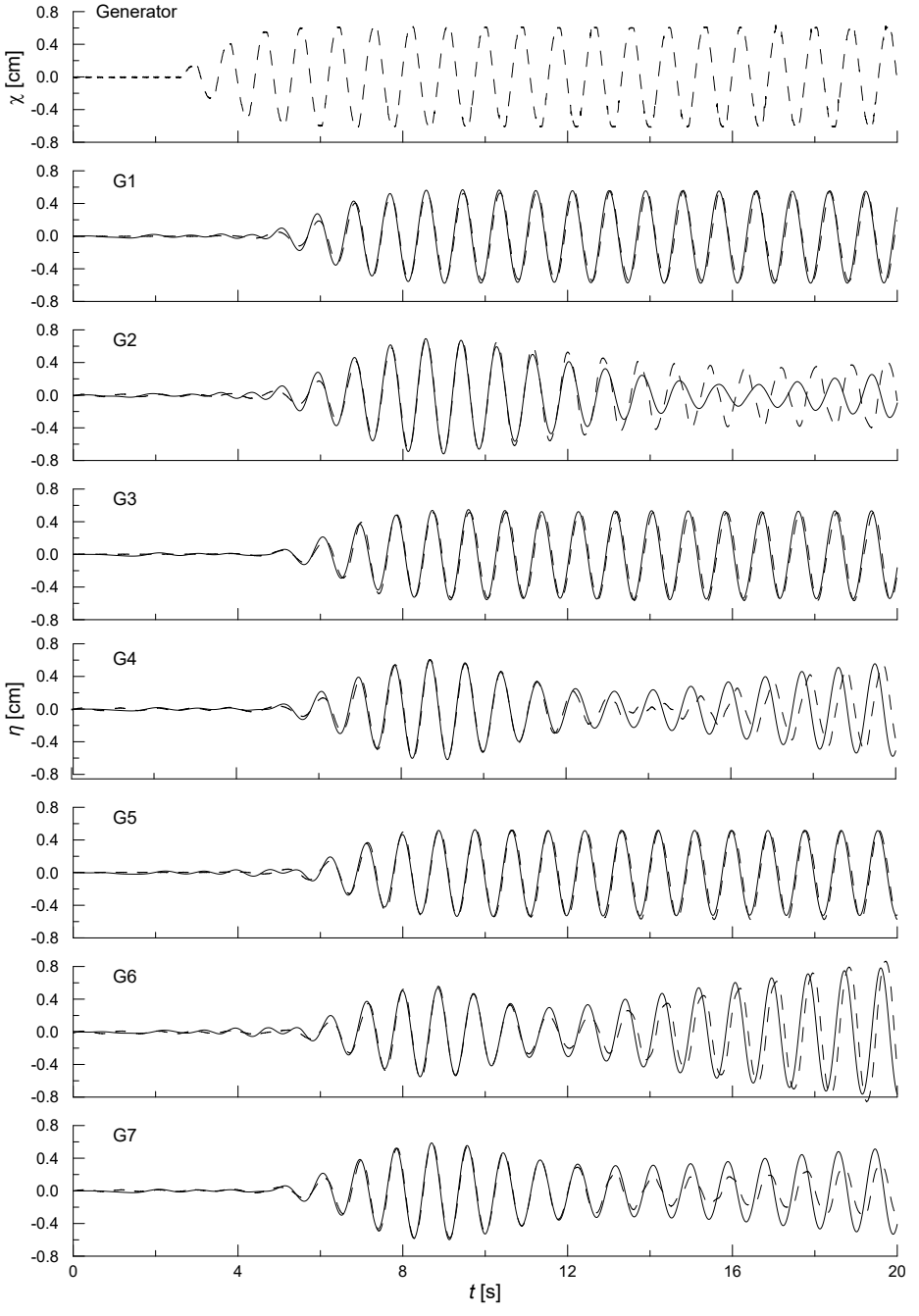

FIG. 11a. Predicted and measured free-surface elevation for $L/h = 3$, — theoretical results, --- experimental data.

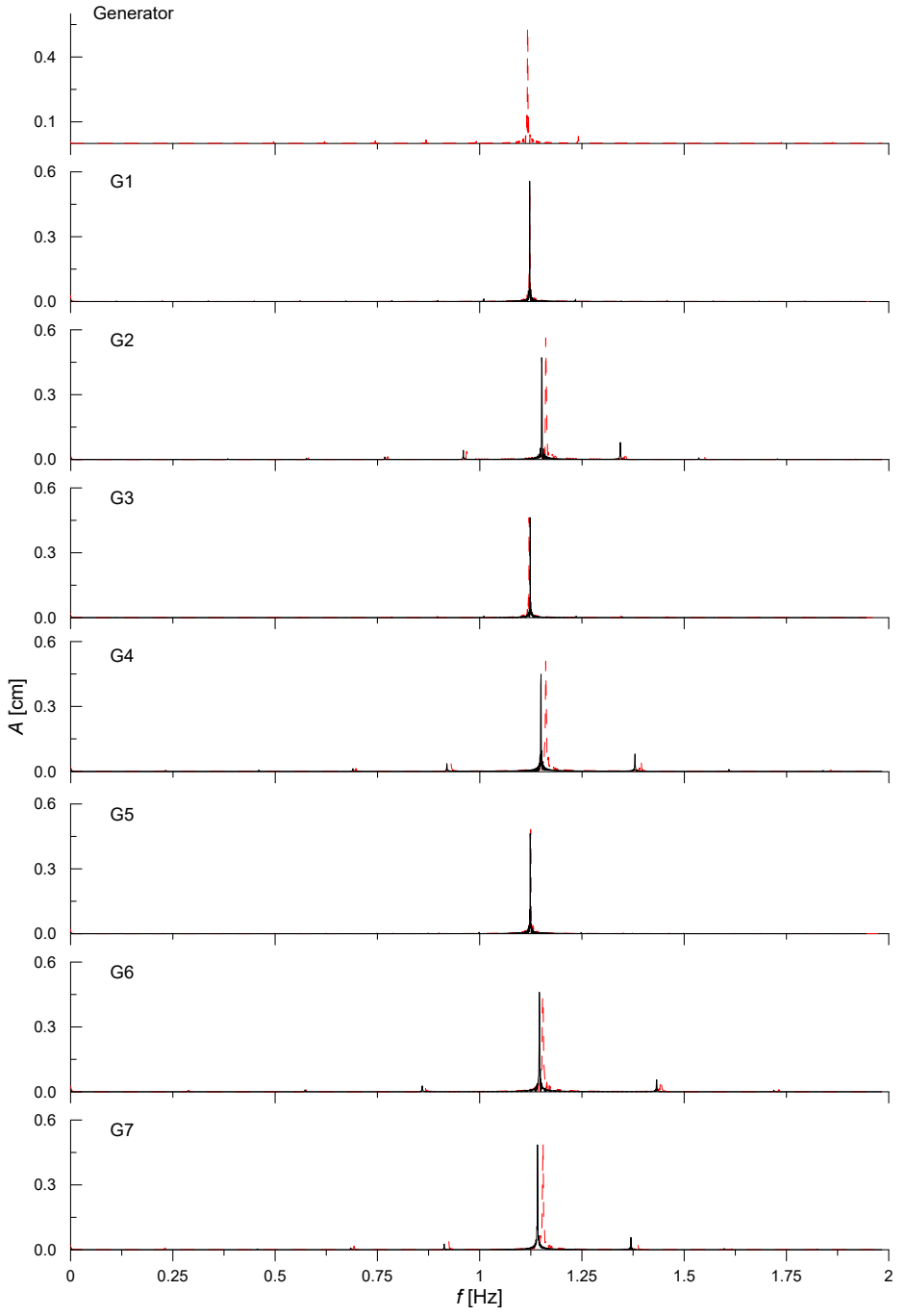

Fig. 11b. Amplitudes of Fourier series for $L/h = 3$, — theoretical results, --- experimental data.

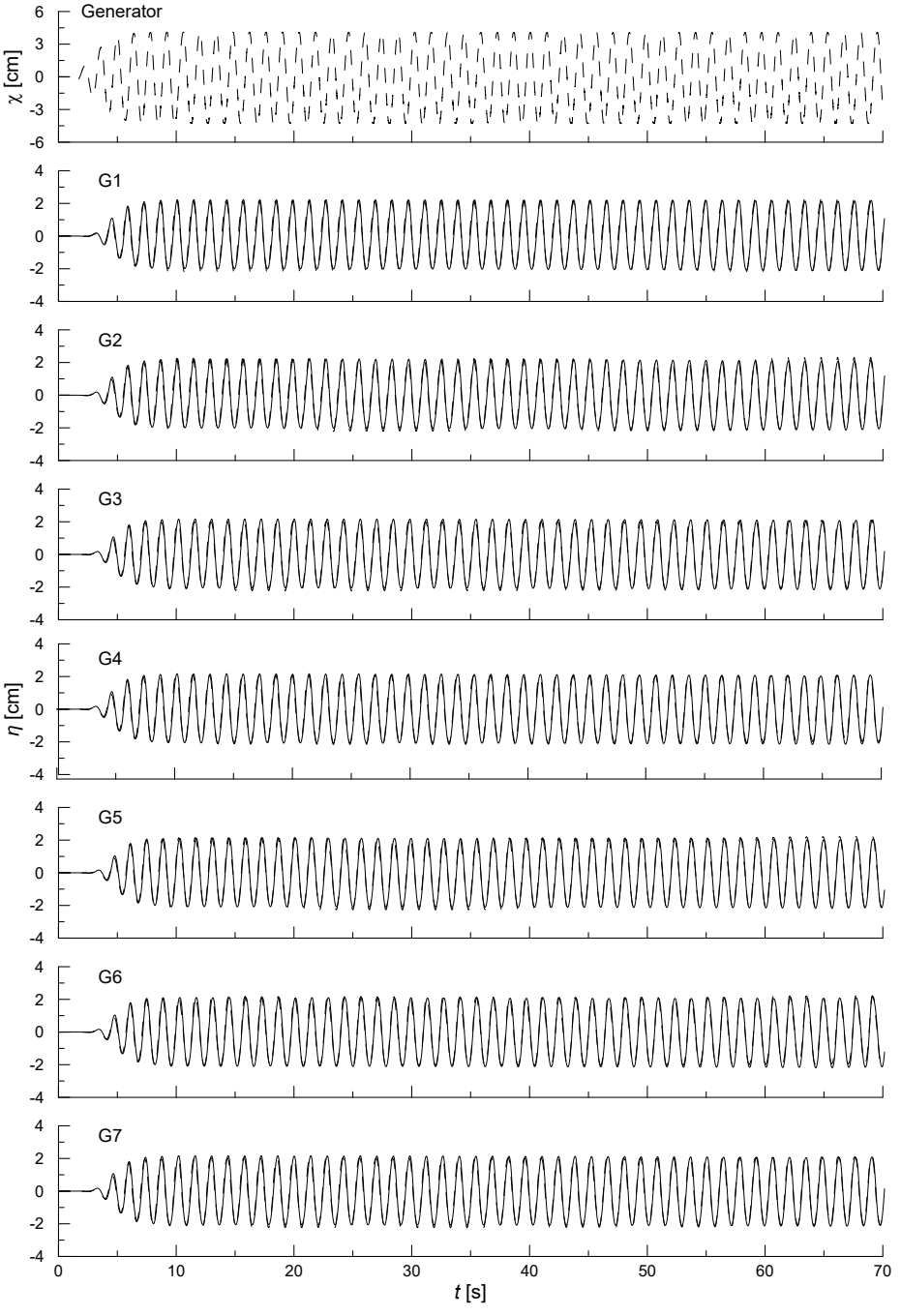

FIG. 12a. Predicted and measured free-surface elevations for a long wave train, $L/h = 6$, — theoretical results, --- experimental data.

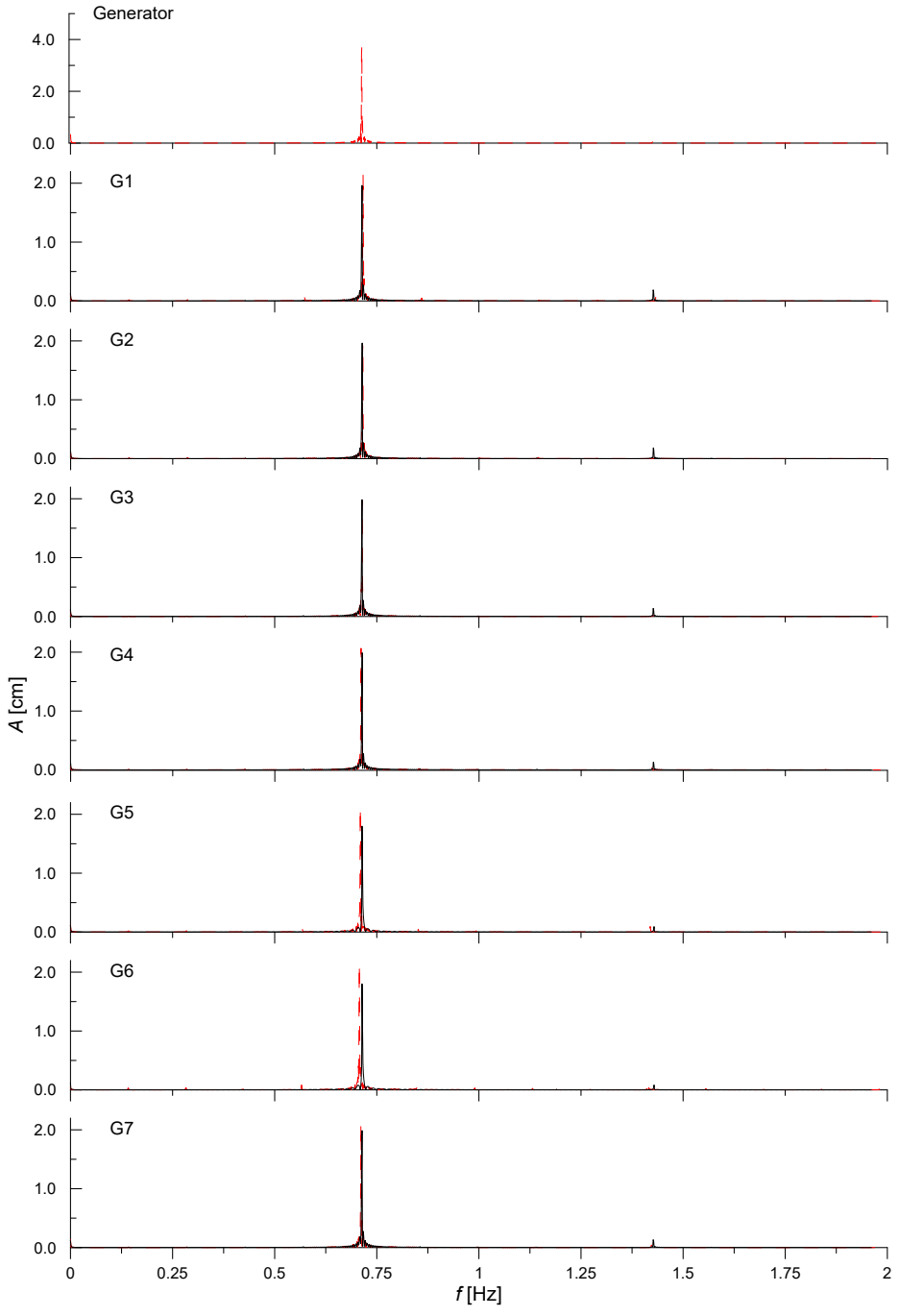

Fig. 12b. Amplitudes of Fourier series for a long wave train, $L/h = 6$, — theoretical results, --- experimental data.

The discrepancies observed between theoretical results and experimental data are probably due to inaccuracies in a mechanical system as well as a leakage and a wave damping around a moving wavemaker paddle that were not modeled with sufficient accuracy. Inaccuracy in a mechanical generation system including a leakage and a wave damping around a wavemaker paddle, become important especially when cross-wave frequency is very close to the basin resonance frequency, as in the case of $L/h = 3$. The modelling of the generation of resonance in the time domain is very sensitive to initial conditions. Small inaccuracy in the mechanical generation system leads to discrepancies between predicted and recorded free surface elevations, especially in the second stage of wave motion due to the accumulation and amplification in time of a small error arising from the inaccuracy in the mechanical generation system.

The developed model and methodology are very attractive from a theoretical and practical point of view and can be applied to verify advanced three-dimensional nonlinear wave models as well as to conduct accurate investigations on nonlinear wave propagation and transformation in channels and harbour basins, navigational channels, interactions of nonlinear cross-waves with structures, nonlinear cross-wave loads on ships and maritime structures, formation and development of cross waves, formation of wave resonance, creation and transformation of seiches, development of sloshing phenomena, etc.

5. Conclusions

Theoretical investigations were conducted to study the generation of transient nonlinear water waves by a novel side-hinged paddle wavemaker. A semi-analytical nonlinear solution is achieved by applying eigenfunction expansions and FFT. The derived solution is applied to study the features of nonlinear waves generated by a side-hinged paddle wavemaker including the effect of the frequency and the magnitude of wavemaker oscillations on the generation and propagation of nonlinear waves as well as the formation and development of cross waves.

The results show that for waves of very low steepness the nonlinear terms in the free-surface boundary conditions and the kinematic wavemaker boundary condition are of secondary importance, so the contribution of nonlinear wave effects may be neglected and a linear wave theory may be applied to predict the generation of waves by a side-hinged paddle wavemaker. For larger amplitudes of wavemaker displacements, generated waves are higher and the contribution of nonlinear wave effects cannot be neglected. The nonlinear effects imply the modification of wave profiles so that wave troughs are flattered and crests are getting steeper and cause that the interactions between waves in a wave train are becoming more and more important, and are no longer negligible. The analysis

shows that the discrepancies between wave profiles predicted by applying the linear and nonlinear models increase with increasing wavelength and become significant for long waves which profiles become more and more cnoidal. The results also show that the application of the nonlinear model has a significant effect on the shape of a wave spectrum. The results show that a train of originally very narrow-banded waves changes its one-peak spectrum to a multi-peak one when a wavemaker displacement increases.

The derived model provides insight into the effects of nonlinear terms in the free-surface boundary conditions and in the kinematic wavemaker boundary condition on a final solution. This problem is of significant importance for the interpretation and understanding of nonlinear wave phenomena implied by mechanically generated waves which are specific-type waves subject to nonlinear effects arising from the free-surface boundary conditions and the kinematic wavemaker boundary condition. The analysis shows that the contributions of nonlinear terms present in the kinematic wavemaker boundary condition are of secondary importance for a final solution. The low effects of the nonlinear terms in the kinematic wavemaker boundary condition on a final solution are the advantage of a side-hinged paddle wavemaker because nonlinear wave effects disturb physical modeling of numerous processes including wave-induced transport, sediment transport, etc. Often, nonlinear wave effects may drastically disturb or even exclude physical modeling conducted in wave flumes or wave basins by altering or completely deforming a designed wave spectrum.

The analysis shows that there is a fairly good agreement between theoretical results predicted by the derived nonlinear model and the experimental data. A reasonable agreement is observed between predicted and measured time series of the free-surface elevations and the amplitudes of the corresponding Fourier series. The plots also show that wave phases predicted by applying the theoretical model are in reasonable agreement with experimental data. The model predicts fairly well multi-peak spectrums characteristic for nonlinear waves as well as the formation and development of cross-waves. The discrepancies observed between theoretical results and experimental data are probably due to inaccuracy in a mechanical system as well as leakage and wave damping around a wavemaker flap that were not modeled with sufficient accuracy.

The investigations show that a side-hinged paddle wavemaker is an attractive wave generation system. The simple and reliable boundary condition at the paddle enables verification of advanced three-dimensional nonlinear models and accurate physical modeling of many phenomena where high accuracy or details of incoming wave properties are important. The wavemaker proposed in our study may be installed basically in all laboratories by changing the hinge of a flap.

Acknowledgements

Financial support for this study was partially provided by the MuWin project, MarTERA4/1/9/MuWin/2023. The financial support is gratefully acknowledged.

References

1. T.H. Havelock, *Forced surface-wave on water*, Philosophical Magazine, **8**, 51, 569–576, 1929, doi: 10.1080/14786441008564913.
2. F. Biesel, F. Suquet, *Laboratory Wave Generating Apparatus*, Project Report No. 39, St. Anthony Falls Hydraulic Laboratory University of Minnesota, Minneapolis, Minnesota, USA, 1953.
3. J.M. Hyun, *Theory for hinged wavemakers of finite draft in water of constant depth*, Journal of Hydronautics, **1**, 10, 1976, doi: 10.2514/3.63046.
4. R.G. Dean, R.T. Dalrymple, *Water Wave Mechanics for Engineers and Scientists*, Englewood Cliffs, Prentice-Hall, New York, USA, 1984.
5. F. Ursell, R.G. Dean, Y.S. Yu, *Forced small amplitude waves: a comparison of theory and experiment*, Journal of Fluid Mechanics, **7**, 33–52, 1960, doi: 10.1017/S0022112060000037.
6. C.J. Galvin, *Wave-height Prediction for Wave Generators in Shallow Water*, Technical Memorandum No. 4, pp. 1–20, U.S. Army Corps of Engineers, Washington, DC, USA, 1964.
7. T. Keating, N.B. Webber, *The generation of periodic waves in a laboratory channel; a comparison between theory and experiment*, Proceedings of the Institution of Civil Engineers, **63**, 819–832, 1977, doi: 10.1680/iicep.1977.3078.
8. N.H. Patel, P.A. Ionnaou, Comparative *performance study of paddle and wedge-type wave generators*, Journal Hydronautics **14**, 5–9, 1980.
9. Y. Goda, T. Kikuya, *The generation of water waves with vertically oscillating flow at channel bottom*, Rep. 9. Port and Harbour Technical Research Institute, Ministry of Transportation, Japan, 1964.
10. R.H. Multer, C.J. Galvin, *Secondary waves: periodic waves of non-permanent form*, Abstract, EOS, **48**, 1967.
11. Y. Iwagaki, T. Sakai, *Horizontal water particle velocity of finite amplitude waves*, Coastal Engineering Proceedings, **1**, 12, 19, 1970, doi: 10.9753/icce.v12.19.
12. P. Fontanet, *Theorie de la generation de la houle cylindrique par un batteur plan*, La Houille Blanche, **16**, 1, 3–31, 1961.
13. O.S. Madsen, *On the generation of long waves*, Journal of Geophysical Research, **76**, 8672–8683, 1971, doi: 10.1029/JC076i036p08672.
14. R.T. Hudspeth, W. Sulisz, *Stokes drift in two-dimensional wave flumes*, Journal of Fluid Mechanics, **230**, 209–229, 1993, doi: 10.1017/s0022112091000769.

15. W. Sulisz, R.T. Hudspeth, *Complete second-order solution for water waves generated in wave flumes*, Journal of Fluids and Structures, **7**, 3, 253–268, 1993, doi: 10.1006/jfls.1993.1016.

16. W. Li, A.N. Williams, *Second-order waves in a three-dimensional wave basin with perfectly reflecting sidewalls*, Journal of Fluids and Structures, **14**, 4, 575–592, 2000, doi: 10.1006/jfls.1999.0285.

17. H.A. Schaffer, C.M. Steenberg, *Second-order wavemaker theory for multidirectional waves*, Ocean Engineering, **30**, 10, 1203–1231, 2003, doi: 10.1016/S0029-8018(02)00100-2.

18. S.A. Hughes, *Physical models and laboratory techniques in coastal engineering*, Word Scientific Publishing, Singapore, 981-02-1540-1, 1993, doi: 10.1142/2154.

19. J.V. Wehausen, *Surface Waves*, in: *Handbuch der Physik 9*, Springer-Verlag, Berlin, pp. 446–778, 1960.

20. B. Kinsman, *Wind Waves*, Prentice-Hall, Englewood Cliffs, New Jersey, 1965.

21. W. Sulisz, M. Paprota, *Modeling of the propagation of transient waves of moderate steepness*, Applied Ocean Research, **26**, 137–146, 2004, doi: 10.1016/j.apor.2005.03.001.

22. W. Sulisz, M. Paprota, *Generation and propagation of transient nonlinear waves in a wave flume*, Coastal Engineering, **55**, 4, 277–287, 2008, doi: 10.1016/j.coastaleng.2007.07.002.

23. L.V. Kantorovich, V.I. Krylov, (translated by Curtis D. Benster), *Approximate Methods of Higher Analysis*, Groningen: Noordhoff, Libraries Australia, ID: 2549557, 1958.

24. W.H. Press, B. Flannery, S.A. Teukolsky, W.T. Vetterling, *Numerical Recipes*, Cambridge University Press, Cambridge, 1988.

25. W. Sulisz, *Numerical modeling of wave absorbers for physical wave tanks*, Journal of Waterway, Port, Coastal and Ocean Engineering, ASCE, **129**, 1, 5–14, 2003, doi: 10.1061/(ASCE)0733-950X(2003)129:1(5).

26. M. Paprota, W. Sulisz, *Improving performance of a semi-analytical model for nonlinear water waves*, Journal of Hydro-environment Research, **22**, 38–49, 2019, doi: 10.1016/j.jher.2019.01.002.

Received September 7, 2022; revised version March 8, 2023.
Published online May 5, 2023.